 CMES, vol.20, no.1, pp.11-20, 2007

FEM Analysis of Knife Penetration through Woven Fabrics

L. Wang[1], S. Zhang, W. M. Gao and X. Wang

Abstract: In this paper, the penetration of a knife through a plain woven fabric is simulated with the finite element method to understand the process of stabbing and the mechanism of fiber breakage. The model focuses on the study of the deformation of individual yarns, and the effects of their material properties and fabric structure on the stabbing resistant force. The performance of the fabric is analyzed as a response of stabbing and the stress distributions in yarn transverse and longitudinal directions. An equation derived from energy and momentum conservations of the knife is proposed to predict the depth of the knife penetration.

Keyword: Stab resistance, soft body amour, FEM analysis, fabric structure.

Nomenclature

Symbol	Denotes
a	yarn cross-section parameter (related to width)
b	yarn cross-section parameter (related to height)
c	distance between yarns
$[C]$	matrix of material properties
G	shear modulus
Ex	Young's Modulus
Fs	static coefficient of friction
H	dropping height of knife
L	depth of knife penetration
m	mass of knife
υ	velocity of knife
λ	poisson ratio
ε	strain
δ	stress

[1] lijing@deakin.edu.au Centre for Material and Fibre Innovation, Geelong Technology Precinct (GTP) Deakin University, Geelong VIC 3217, AUSTRALIA

1 Introduction

The penetration of knives or other edged weapons through soft body amours is a complex and inherently variable event. However, due to the complexity of both the stabbing process and textile reinforcing architectures, the mechanisms that control and affect the performance of a particular system are normally considered to be unique to the particular knife-fabric combination. Homogenization concepts such as the direct average method of stress and strain, the direct average method of strain energy density and the two-scale expansion method, have been widely applied to fibre composites for effective prediction of the effective macroscopic properties of composites [Haasemann et al (2006); Yang and Becker (2004)]. Different homogenization techniques have also be commonly used to model a woven fabric as a nonlinear material with a standard elastic-plastic response, which normally comes from studying the effective material properties of a typical unit cell of woven fabrics [Agarwal and Bhandarkar (1996); Chou (1992); Kwon and Roach (2004); Nadler and Steigmann (2003); Dasgupta, Sun, Lin and Hu (2001), Bohm et al (2004)]. However, for a stab-resistant woven fabric, its mechanical behavior is dominated by the kinematics of the constituents on the microscopic scale [Ballhause et al (2006)] and structural failures usually occur as a result of localized yielding and fracture. The homogenization techniques cannot be used to study the mechanism of failure, especially, the process of the penetration of a knife through a woven fabric, where the knife directly interacts with only a few yarns. Moreover, the effects of textile architecture and yarn-to-yarn friction have been neglected in previous modeling works [Cunnif (1992); Karaoglan and Noor (1997)]. In fact, knowledge of yarn-and-yarn, and

yarn-and-knife interactions are essential to understanding the mechanism of yarn breakage. Therefore, in order to predict the initiation of failure and the progression of failure after initiation, it is necessary to understand the processes of stabbing at the fiber/yarn level, and sequentially, how these processes influence the global material behavior.

In the present work, the stabbing processes are studied at the yarn level with the finite element method (FEM). A plain woven fabric is used as the stab-resistant material and a knife is created based on NIJ Standard. The stab-resistant behavior of the fabric modeled with a simple geometrical shape is analyzed as a response of the knife penetration. An equation derived from the energy and momentum conservations of the knife is proposed to predict the depth of the knife penetration.

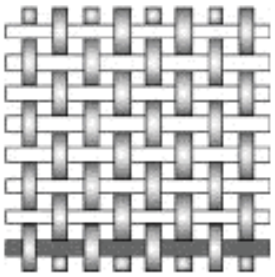

Figure 1: Structure of a plain woven fabric

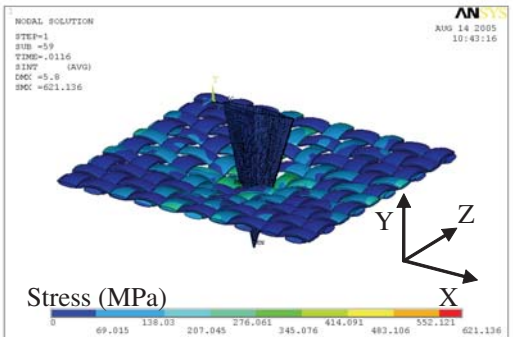

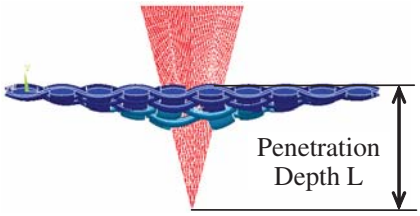

Figure 2: An example of knife penetrating a woven fabric 5.3 mm

2 Modeling

2.1 Textile Structure – Woven Fabrics

Woven fabrics are generally fabricated by interlacing yarns. There are hundreds of possible interlace combinations to make a fabric. Fabrics can be divided into biaxial and triaxial woven structures according to in-plane yarn orientation. The most common constructions are plain (Fig. 1), twill, basket, satin, and leno weaves. In the present work, the biaxial plain woven fabric, as shown in Figures 1 and 2, is used, which is fabricated by the interlacing of warp (0°) and weft (90°) yarns. Thus, orthotropic strength properties of yarns can be considered, e.g. with the through-thickness direction Y and the two yarn directions X and Z (Fig. 2). The stress-strain relationship can be generally written as Equation 1.

$$\langle \varepsilon \rangle = [C] \langle \sigma \rangle \tag{1}$$

With $\langle \sigma \rangle = \langle \ \sigma_{xx} \quad \sigma_{yy} \quad \sigma_{zz} \quad \sigma_{xy} \quad \sigma_{xz} \quad \sigma_{yz} \ \rangle$ and $\langle \varepsilon \rangle = \langle \ \varepsilon_{xx} \quad \varepsilon_{yy} \quad \varepsilon_{zz} \quad \varepsilon_{xy} \quad \varepsilon_{xz} \quad \varepsilon_{yz} \ \rangle$.

For general orthotropic, the material properties $[C]$ can be expressed as:

$$\begin{bmatrix} \frac{1}{E_x} & \frac{-\lambda_{yx}}{E_y} & \frac{-\lambda_{zx}}{E_z} & 0 & 0 & 0 \\ \frac{-\lambda_{xy}}{E_x} & \frac{1}{E_y} & \frac{-\lambda_{zy}}{E_z} & 0 & 0 & 0 \\ \frac{-\lambda_{xz}}{E_x} & \frac{-\lambda_{yz}}{E_y} & \frac{1}{E_z} & 0 & 0 & 0 \\ 0 & 0 & 0 & \frac{1}{G_{xy}} & 0 & 0 \\ 0 & 0 & 0 & 0 & \frac{1}{G_{xz}} & 0 \\ 0 & 0 & 0 & 0 & 0 & \frac{1}{G_{yz}} \end{bmatrix}$$

The properties of yarns are fundamental in the present modeling. The most advantage of this model is that it can isolate the effect of specific geometric factors and material properties. For example, the stab resistant force of a woven fabric can be evaluated for different yarn shapes and wo-

ven structures, keeping the same material properties of fibers and volume fraction of the woven fabric.

2.2 Geometrical definition of a plain woven fabric

A fabric is assumed to form with the same pattern of yarn configuration in both X and Z directions. Fig. 3 shows a repeating unit. The cross-section of a yarn can be approximated as an ellipse. The structure of the plain woven fabrics can be geometrically determined by three parameters, a, b and c. Parameters a and b mainly define the cross-section size of yarns, and c reflects the distance between yarns. Other parameters in Fig. 3, which are used in creating the fabric model, can be deduced from the three parameters. They are:

$$R = \frac{(a+c)^2 - b^2}{2b} \tag{2}$$

$$r = R - \sqrt{a^2 + (R-b)^2} \tag{3}$$

$$\alpha = \arcsin\left(\frac{a}{R-r}\right) \tag{4}$$

$$\beta = \arcsin\left(\frac{a+c}{R+b}\right) \tag{5}$$

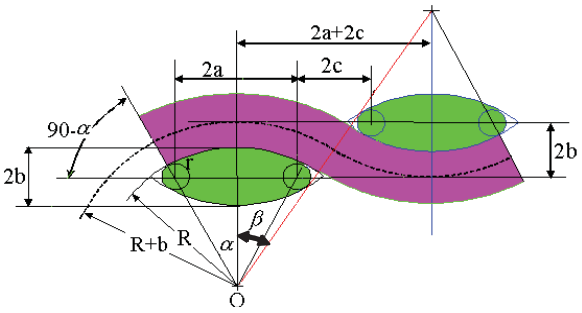

Figure 3: A repeating unit of a plain weave fabric

The cross-sectional area of a yarn can be calculated with Equation (6).

$$A = \pi r^2 + 2\alpha(R^2 - r^2) - 2a(R-b) \tag{6}$$

The volume fraction of yarns, which is defined by Equation (7), is also an important parameter in textile composite structural performance, and has been used by many researchers [Pastore and Ko (1990); Vandeurzen (1998); Tan et al (1997)] to describe the woven fabrics in analyzing the effect of waving structures. For the woven fabric used in the present simulation, the yarn volume fraction is given by Equation (8).

$$f_{yarns} = \frac{V_{yarns}}{V_{fabic}} \tag{7}$$

$$f_{yarns} = \frac{\beta A(R+b)}{4b(a+c)^2} \tag{8}$$

The basic properties of the constituent material involved in $[C]$ and variables used in the simulation are listed in 2.3. In this work, the yarn volume fraction is considered as a structural parameter of woven fabric when comparing the simulation results for different woven fabric structures. The effects of elastic modulus, frictional factors between yarns, and the yarn volume fraction on the resistant forces are studied.

2.3 Stab modeling

The knife was assumed to be a projectile that impacts on the woven fabric at 0° of incidence angle. It was modeled as a rigid material. The structure and structural parameters are shown in Fig. 4.

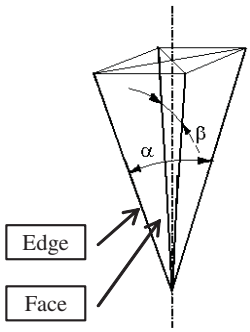

Figure 4: The schematic geometry of knife ($\alpha = 23°$ and $\beta = 5.16°$) [NIJ Standard–0115.00]

Static simulations were performed for the penetration of the knife through the plain-woven fabric. The force and energy transfer and interactions between the knife and yarns during impacting, the relationships between the penetrating depth (L in

Table 1: The properties of the constituent yarn (Kevlar) and the structural parameters of the fabric

Parameter		Value
Basic Properties	$E_y = E_z$ (Gpa)	15
	λ_{xy}	0.25
	$\lambda_{yz} = \lambda_{xz}$	0.245
	G_{xy} (Gpa)	5
	$G_{yz} = G_{xz}$ (Gpa)	2
	a (mm)	0.5
	b (mm)	0.2
Variables	Ex (GPa)	10, 15, 18, 30, 60, 100, 150, 180
	Fs	0.2, 0.25, 0.3, 0.35
	c (mm) ($f_{yarns}(\%)$)	0.2 (64.2), 0.4 (58.6), 0.46 (56.6), 0.6 (51.9)

Fig. 2) and the interactive forces, and the properties of yarns and the textile structures were studied. The stab resistant force F_t can be described as a function of knife penetrating depth L_t at the impacting time t, as expressed in Equation (9).

$$F_t = f_F(L_t) \tag{9}$$

For the knife with a mass of m and a velocity of υ, its kinetic energy is $0.5\, m\upsilon^2$ and its momentum is $m\upsilon$. Since F_t is the vertical force of the knife at impacting time t, Equation (10) exists (ignoring the fabric momentum).

$$F_t dt = d(m\upsilon) \tag{10}$$

At time t, the displacement of knife can be expressed as

$$dL = \upsilon dt \tag{11}$$

Substituting F_t (Equation 9) and dt (Equation 11) into Equation (10) gives Equation (12)

$$f_F(L_t)dL = m\upsilon d\upsilon \tag{12}$$

For the knife with an initial velocity of υ_0 and a penetration depth of 0, integrating Equation (12) gives the knife energy conservation Equation (13).

$$\int_0^L f_F(L_t)dL = \frac{1}{2}m\upsilon_0^2 \tag{13}$$

Once the function $f_F(L_t)$ is given or the relation of the knife penetration depth and the resistant force is tabulated, the stabbing depth can be calculated for a given energy of a dropping knife.

2.4 FEM Analysis

Three-dimensional finite element analysis was carried out to evaluate the resistance force of the plain-woven fabric described in Fig. 3. The simulation was implemented with ANSYS-LS_DYNA. The yarns were meshed with an 8-node brick element (Solid 164). Fig. 5 shows the geometry and the mesh of a woven fabric unit. The knife was considered as a rigid body and then the shell element of Shell 163 was used to mesh the surface of the knife. Then total elements of about 31000 were created for the woven fabric. The ends of each yarns were fixed during knife penetration, i.e. the displacements of the nodes at the end of each yarn (four sides of the fabric) are 0, hence $dx = dy = dz = 0$. These boundary conditions were used for all the runs in the present work.

Figure 5: FE Model of a woven fabric unit

3 Results and Discussion

3.1 The process of stabbing

Based on the FE model in Fig. 5, simulations were performed for large displacements and finite strains. Fig. 6 shows that the fabric exhibits a complex mechanical behavior and nonlinear response, even in the elastic region of deformations, due to the architecture of the woven fabric and the interactions between yarns. It can be seen from Fig. 6 that the resistance force nonlinearly increases with the penetration depth of the knife. The higher the Young's Modulus of the constituent yarn, the better the fabric resists to knife penetration. For a given stab-resistant capacity (force), an increase in yarn elastic modulus results in reduced knife penetration depth, hence better stabbing protection.

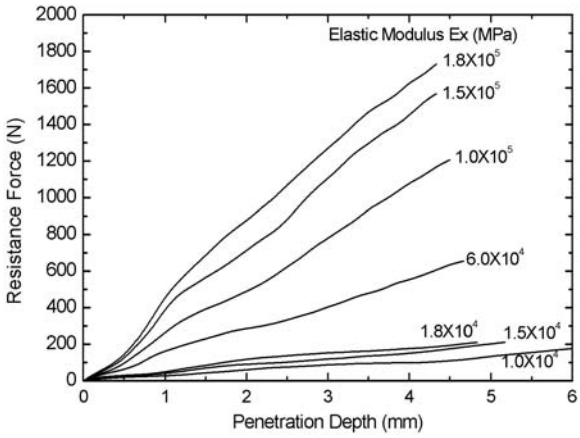

Figure 6: Effect of yarn elastic modulus on the stab-resistant performance (Fs=0.25, c=0.4 mm)

When the fabric is deformed by the knife penetration, it exhibits a considerable difference in extensive stiffness compared to that of a yarn. Under tensile loading, as yarns are straightening, the fabric stiffness increases.

The nonlinear reaction of the woven fabric to the knife stabbing can be characterized into three periods. Fig. 7 shows an example of the three periods, the typical yarn stress and the deformation of the fabric at different knife penetration depth. In the first period, the knife starts to push the yarns and compact them gradually. The yarns in contact with the knife move in the stabbing direction. The penetration depth is up to 1 mm and the distance between parallel yarns, c, remains in its initial value of 0.4 mm. The increase of stab-resistant force is due to the straightening of yarns and the compaction of the woven fabric. As the straightening of yarns increases the stiffness of the overall woven fabric, the energy dissipation is faster at the initial stage of penetration.

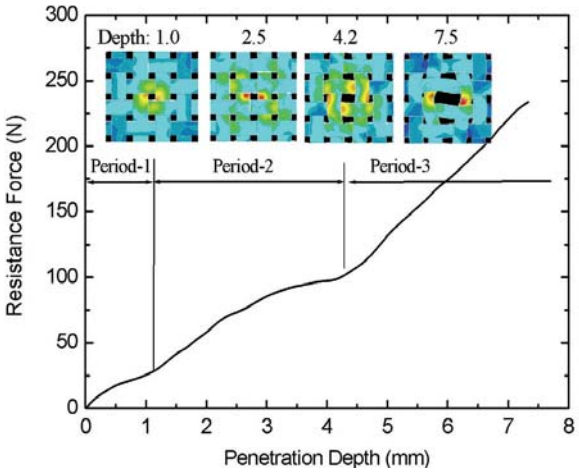

Figure 7: Variation of stab resistant force $Ex = 1 \times 10^4$ MPa, $Fs = 0.25$, $c = 0.4$ mm)

The second period begins when the two warp yarns in contact to the knife edges begin moving, and finishes before the weft yarns come in contact with the knife face. The contacting yarns transversely move about 0.2 mm, and the corresponding depth of knife penetration is about 3∼3.5 mm. During this period, some yarns are pushed closer together and the friction between yarns absorbs some knife energy. Therefore, the resistant force rises slowly compared to the third period, which leads to a higher ratio of the resistant force to the penetration depth (Figures 6 and 7). During the third period, the compactness between yarns results in higher elastic modulus and stiffness of the woven fabric around the knife, and fabric damage will occur.

In order to better understand stab-resistant behavior, the deformation of structure and the stress distribution of the plain-woven fabric were analyzed at different penetrating depths as shown in Fig. 8.

The positions with maximum stress in the yarns in contact with the knife edges are close to the crossover points, where the warp and weft yarns were on top of each other, at the penetration depth of 5.3 mm (Fig. 8a). They then shift to the yarn and knife edge contact points, and the area with very high stress becomes smaller at the penetration depth of 8.5 mm (Fig. 8b). This suggests that:

- the stabbing energy dissipation is lower as the penetration depth increases;
- the shear properties of fibers are more important than their tensile properties because of stress concentration; and
- the damage will start from the individual fibers that come in contact with the knife edges, which will lead to the breakage of a yarn.

Therefore, the knife penetration can be attributed to the fiber breakage resulted from the shearing. This will be used to develop a failure model for simulating the stabbing process in the sequential publications.

Fig. 9 shows the distribution of stress in Yarn-1 (Fig. 8a) at different penetration depths. The fiber with maximum stress occurs close to the point in contact with the knife. At the penetration depth of 2.6 mm, the yarns in contact with the knife edge (line L_3) have a maximum stress. The force impacted on the woven fabric is dispersed through yarns with the progress of stabbing, as shown in Fig. 9b. The stresses of the fibers in the top of the yarn (lines L_1, L_2 and L_3) are approximately the same in Fig. 9b, and the stresses of the fibers at lines L_1 and L_2 are higher than that of fiber at line L_3 in Fig. 9c This suggests that, at the beginning, the penetration of knife through a woven fabric is an "impacting" process. With the further progress of stabbing, the fibers with maximum stress are those that come in contact with the knife at all times (Fig. 9c). In practice, the fiber at line L_3 may have already failed at the penetration depth of 8.5 mm.

It can also been seen that there is a great difference in stress crossing the yarn sections close to

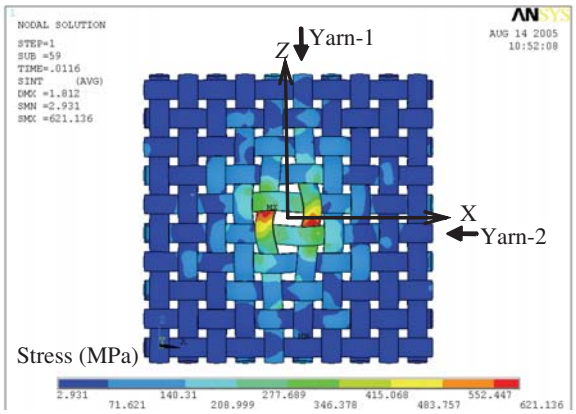

(a) Penetration depth = 5.3 mm

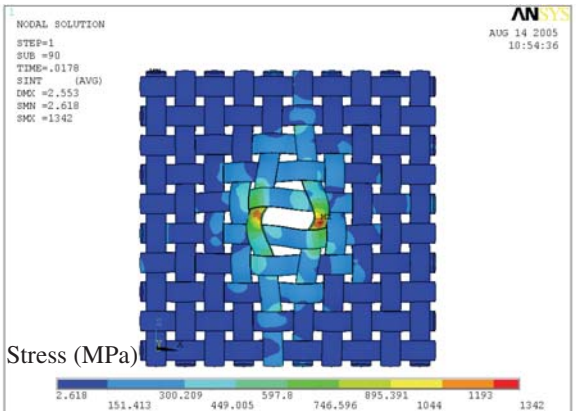

(b) Penetration depth = 8.5 mm

Figure 8: Fabric deformation and stress ($E_x = 1 \times 10^4$ MPa)

the knife (position = 0 in Fig. 9) and to the yarn crossover points at all times, especially between the top and bottom fibers. The fibers at the centre of the yarn (line L_5) have lower stress. This can be attributed to the bending of these fibers.

The stress of the fibers close to the knife is so high that it is about three times of the stress of the fibers away from the knife. Therefore, the stress concentration builds up and the fiber breakage would occur at the fiber-knife contacting position. The local properties of a woven fabric are more important than the elastic modulus of the yarns composing the fabric. The stress concentration and the fiber breakage are different to that of ballistic impact, where the stress concentrations and the yarn breakage occurs not only under the projectile penetrating the target material, but also at the

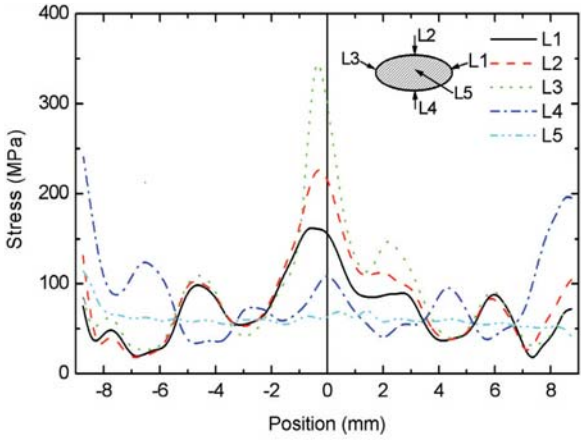

(a) Penetration depth = 2.6 mm

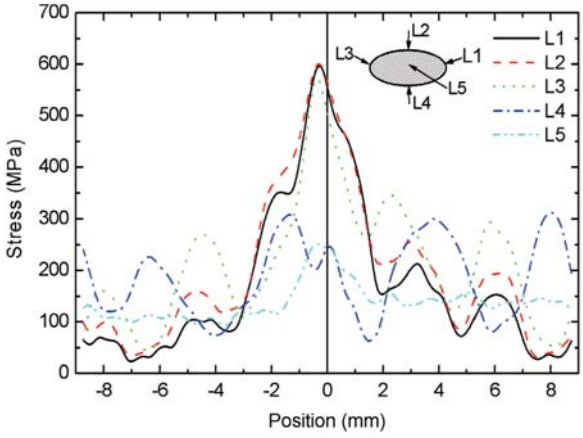

(b) Penetration depth = 5.3 mm

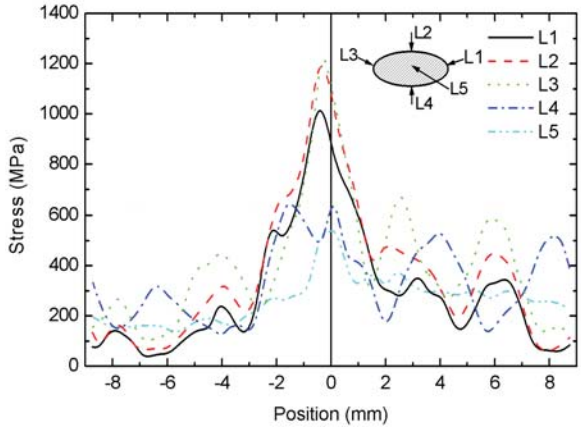

(c) Penetration depth = 8.5 mm

Figure 9: Stress distribution in Yarn-1 (Fig. 8a) at different penetration depths

yarn crossover points exceeding the strength of material, while the knife penetration results from fiber breakage by cutting. The difference in fabric damage will lead to different means to reinforce woven fabrics. Further approach should be able to address particular failure modes using detailed finite element modeling of textile reinforcing structures.

Fig. 10 shows the stress distribution in Yarn-2. Comparing Fig. 9 with Fig. 10, it can be seen that the stress on Yarn-2 is much lower than that on Yarn-1. The maximum stress on Yarn-2 is about half of that on Yarn-1 and occurs at the crossover point. Although woven architecture could absorb a large amount of strain energy, the stab resistant fabric show less efficient as the local deflections are very large and the overall strain along the yarn length is small. This suggests that energy is transferred slowly through the material system.

The strain concentrations in Yarn-1 and Yarn-2 are similar to the distribution of stress as shown in Figure 9 and 10, respectively, due to the assumption of elastic material of the yarns in the present model.

3.2 The influence of fabric properties

3.2.1 Elastic modulus

As discussed earlier, a higher modulus of yarns gives a higher stiffness in the initial structural response of stabbing and a higher resistant force to knife (Fig. 6). The simulations show that the resistant force increases linearly with the elastic modulus of the yarns, as shown in Fig. 11.

Considering the fact that the damage of woven fabrics results from the shearing breakage of fibers, the fibers in a yarn may have already failed by the time the stress of the yarn reaches the tensile failing value. Therefore, the effective Young's modulus of the yarn is a function of the number of broken fibers, and the stress in the yarn will decrease as fibers stretch/cut to break. This will lead to the nonlinear dependence of the resistance force on the elastic modulus of fibers. This will be studied in the future.

3.2.2 Frictional coefficient

Compared to the impact of a projectile on a woven fabric, the frictions between yarns, and between

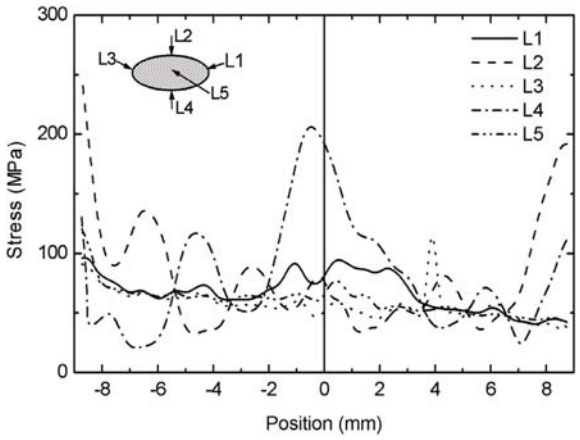

(a) Penetration depth = 2.6 mm

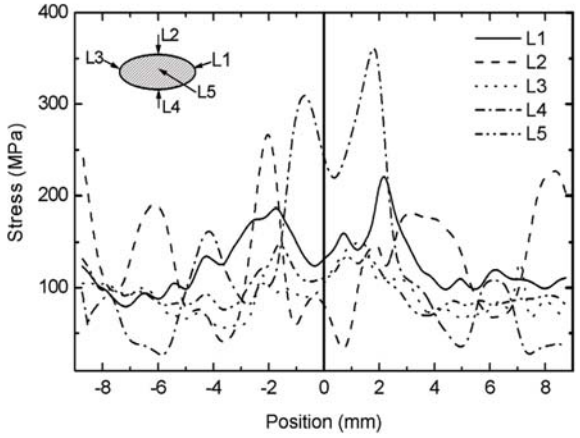

(b) Penetration depth = 5.3 mm

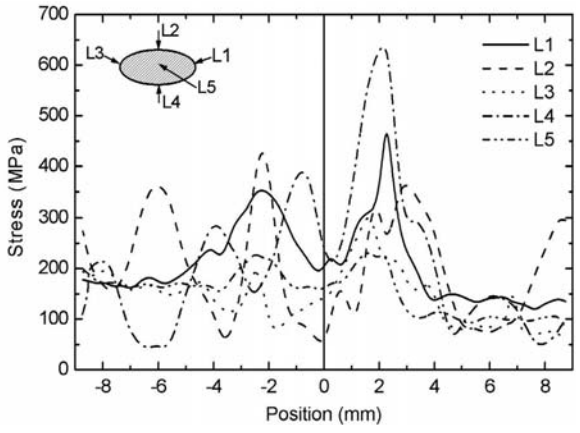

(c) Penetration depth = 8.5 mm

Figure 10: Stress distribution in Yarn-2 (Fig. 8a) at different penetration depths

yarns and knife are more significant, because the component of the interacting force between the

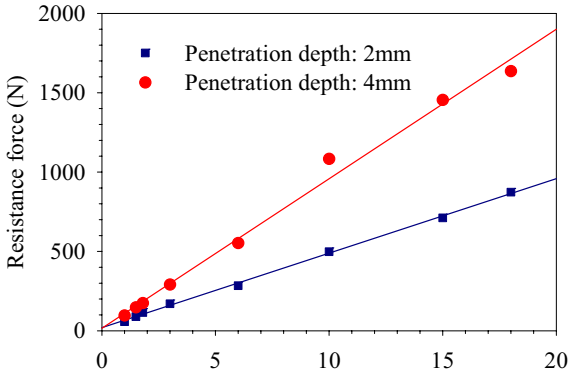

Figure 11: Variation of resistance force with elastic modulus (Fs=0.25, c=0.4 mm)

knife and the woven fabric in plain is much higher than the normal component of the force to the woven fabric, i.e., than the resistance force. Therefore, a high friction can increase transversal resistance force and can lead to decreased deformation of woven fabrics. The relationship between the resistance force and the friction coefficient for the plain woven fabrics can be quantified with Fig. 12. It can be found that the effect of the frictional coefficient on the resistance force at larger penetration depth is more significant.

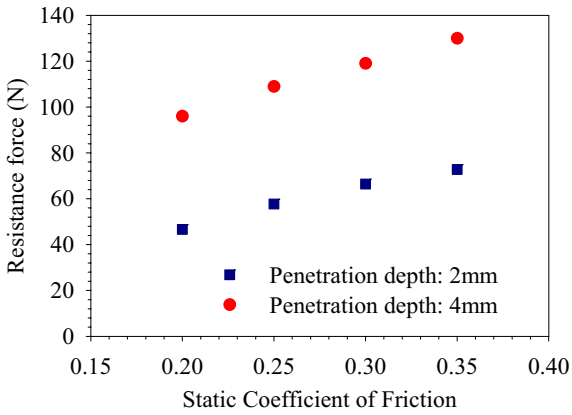

Figure 12: Variation of resistance force with coefficient of friction ($Ex = 4 \times 10^4$ MPa, c=0.4 mm)

The friction between yarns is also one of the important factors which cause the non-linearity between the resistance force and the elastic moduli. The modeling predicts stronger non-linearity for higher frictional coefficient. This essential non-

linear behavior of yarns with higher frictional coefficient results from the significant increase of the yarn-yarn contacting force during stabbing. The influence of the friction factor on the resistance is also dependent on the structure of the woven fabric. As seen in Fig. 12, the increase in the resistant force at larger penetration depth (4 mm) is faster than that at lower penetration depth (2 mm). At a depth of 4 mm, the yarns are tightened surrounding the knife, leading to a higher yarn volume fraction locally, hence a higher stabbing resistant force.

3.2.3 Fabric structure

Many parameters determine the structure of a woven fabric and affect the structure-property maps of the woven fabric. For example, parameters a, b and c are the main variables and determine not only the structure of the woven fabric used in the present work but also the shape of the yarns. In the following, only the effect of c on the resistance force is studied.

The structural parameter of c mainly determines the undulation of the yarns in the woven fabric. A lower value of c will lead to a higher undulate magnitude. As a result, the undulation will result in the reduction of the effective elastic moduli in both the 0° and 90°, hence an overall decrease in stabbing resistance, as described above. On the other hand, a dense woven fabric can be produced with a lower value of c. The fabric with a high yarn volume fraction leads to an increase in stabbing resistance, as shown in Fig. 13.

As described as Equations (2)∼(5), flattening the yarns decreases the distance between yarns. The modeling results indicated that the woven fabric composed of flattering yarns with lower cross-sectional area has higher resistance, because of the dense composition of the woven fabric. It can be concluded that the effect of the structure of woven fabric on the stabbing resistance is more significant than the shape and size of individual yarns.

3.3 Prediction of penetration depth

The present static modeling can give the relation between the resistance force and the depth of penetration for plain woven fabrics of different material and structural parameters. The results can be applied to calculate the penetration in the view of dynamics. For example, the relationship of the resistant force and the penetration depth in Fig. 7 can be given by Equations (14) and (15). For a penetration depth of within 4 and 13 mm ($4<L<13$), we assumed that the resistance force is linearly dependent on the penetration depth. Beyond the penetration depth of 13 mm, where the yarn reaches its maximum stress of approximately 3GPa, the resistant force (i.e. $F(L)$) is assumed to be a constant as the knife cutting through the fabric.

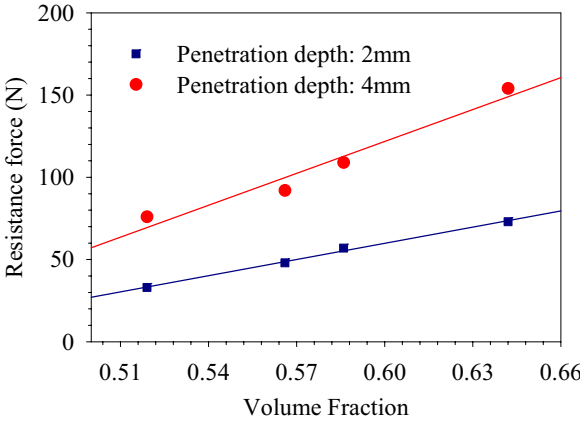

Figure 13: Effect of fabric structure on the stab-resistant force ($Ex = 1 \times 10^4$ MPa, Fs=0.25)

$$f_F(L) = 0.5738 + 45.1L - 19.58L^2 - 28.86L^3 + 52.17L^4 - 30.2L^5 + 8.63L^6 - 1.323L^7 + 0.1044L^8 - 0.00334L^9 \quad (forL \leq 4) \quad (14)$$

$$f_F(L) = 43.7(L - 1.8) (\text{for } 4.0 < L < 13) \quad (15)$$

Based on the above assumptions and Equations (13), (14) and (15), the stabbing depth as a function of the knife energy can be given in Fig. 14. The results will be evaluated with further simulations and experimental data in our further publications.

4 Conclusions

The penetration of a knife through a plain woven fabric was simulated with a finite element method

to improve the understanding of the process of stabbing and the mechanism of fiber breakage. The variation of resistance force during stabling and the stress distributions in transverse and longitudinal yarns were analyzed.

The simulation results show that the fabric exhibits a complex mechanical behavior and nonlinear response even in elastic regions of deformation. The nonlinear reaction of the woven fabric to the knife stabbing can be characterized into three periods.

The penetration of a knife through a woven fabric is attributed to the fiber breakage resulting from the shearing. The fabric structure also significantly affects the stabbing resistant force. The effect of the friction factor on the resistance force is stronger at a larger penetration depth.

The penetration resistance VS depth from the static simulation could be used to predict the penetration depth for knife stabbing.

Acknowledgement: This work was supported by the Victorian Partnership for Advanced Computing e-Research Program Grant Scheme.

References

Ballhause, D.; Konig, M.; Kroplin, B. (2006): Modelling of Woven Fabrics with the Discrete Element Method, *CMC: Computers, Materials & Continua*, Vol. 4(1), pp. 21-30.

Bohm, H. J.; Han, W.; and Eckschlager, A. (2004): Multi-Inclusion Unit Cell Studies of Reinforcement Stresses and Particle Failure in Discontinuously Reinforced Ductile Matrix Composites, *CMES: Computer Modeling in Engineering & Sciences*, Vol. 5(1), pp. 5-20.

.**Chou, T. W.** (1992): *Microstructural Design of Fiber Composites*, Cambridge University Press, Cambridge, UK.

Cunnif, P. (1992): An Analysis of the System Effects in Woven Fabric Under Ballistic Impact, *Textile Research Journal*, vol. 62, pp. 495-509.

Dasgupta, A.; Agarwal, R. K.; Bhandarkar, S. M. (1996): Three-dimensional Modeling of Woven-fabric Composites for Effective Thermo-Mechanical and Thermal Properties, *Composites Science and Technology*, vol. 56, pp. 209-223.

Haasemann, G.; Kästner, M.; Ulbricht, V. (2006): Multi-Scale Modelling and Simulation of Textile Reinforced Materials, *CMC: Computers, Materials & Continua*, Vol. 3(3), pp. 131-145.

Karaoglan, L.; Noor, A. (1997): Frictional Contact/Impact Response of Textile Composite Structure, *Composite Structures*, vol. 37, pp. 269-280.

Kwon, Y. W.; Roach, K. (2004): Unit-Cell Model of 2/2-TwillWoven Fabric Composites for Multi-Scale Analysis, *CMES: Computer Modeling in Engineering & Sciences*, vol.5, no.1, pp.63-72.

Nadler, B.; Steigmann, D. J. (2003): A Model for Frictional Slip in Woven Fabrics, *Comptes Rendus Mecanique*, vol. 331(12), pp. 797-804.

NIJ Standard-0115.00 (2000): *Stab Resistance of Personal Body Armor*, U.S. Department of Justice, Office of Justice Programs, National Institute of Justice.

Pastore, C. M.; Ko, F. K. (1990): Modeling of Textile Structural Composites, Part I: Processing-science Model for Three-dimensional Braiding, *Journal of Textile Institute*, vol. 81(4), pp. 480-490.

Sun, W.; Lin, F.; Hu, X. (2001): Computer Aided Design and Modeling of Composite Unit Cells, *Composites Science and Technology*, vol. 61, pp. 289-299.

Tan, P.; Tong, L.; Steven, G. P. (1997): Modeling for Predicting the Mechanical Properties of Textile Composites-A Review, *Composites Part A*, vol. 28A, pp. 903-922.

Vandeurzen, P. (1998): *Structure Performance Modeling of Two-dimensional Woven Fabric Composites*, Katholieke Universiteit Leuven: Belgium.

Yang, Q. S.; Becker W. (2004): A Comparative Investigation of Different Homogenization Methods for Prediction of the Macroscopic Properties of Composites, *CMES: Computer Modeling in Engineering & Sciences*, Vol. 6(4), pp. 319-332.